Materials Chemistry and Physics 130 (2011) 431–436

Contents lists available at ScienceDirect

Materials Chemistry and Physics

journal homepage: www.elsevier.com/locate/matchemphys

New evidence on the nature of the metastable S″-phase on Al–Cu–Mg alloys

O. Novelo-Peralta, I.A. Figueroa, G. Lara-Rodríguez, G. González *

Instituto de Investigaciones en Materiales, Universidad Nacional Autónoma de México, Circuito Exterior S/N, Ciudad Universitaria, A.P. 70-360, Coyoacán C.P. 04360, D.F., Mexico

ARTICLE INFO

Article history:
Received 2 December 2010
Received in revised form 21 May 2011
Accepted 2 July 2011

Keywords:
Alloys
Precipitation
Electron microscopy (TEM)
Crystal structure

ABSTRACT

Results obtained from high resolution electron microscopy (HRTEM), the resultant fast Fourier transform (FFT) and the simulated electron diffraction patterns (SEDP) presented in this paper provide a better understanding that suggests that there is no S″-phase and that the effects attributed to S″ are explained by consideration of the various variants of the equilibrium S phase on Al–Cu–Mg based alloys (based only on HRTEM analysis). From the 12 orientation variants, only 3 orientations between the matrix and S-phase precipitates were taking into consideration in this study. It was found that the metastable S″-phase could be explained as an orientation variant of the equilibrium S-phase (Al_2CuMg). It is worth mentioning that the third variant has not been reported in the literature using HTREM, therefore, the incorporation of this variant in the analysis provides an alternative explanation for the experimental evidence previously used as support for the S″-phase.

1. Introduction

Al–Cu–Mg alloys have been widely used in the aircraft industry for structural applications because of their combination of high strength and ductility. The mechanical response in these alloys depends on the dispersion of second-phase particles, which act as obstacles for the motion of dislocations [1]. In this sense, Ringer and co-workers [2,3] studied the atomistic-level nanostructure during the early stages of elevated temperature ageing of rapid hardening on Al–Cu–Mg alloys, significant dispersion of small solute cluster which are thought to be responsible for the rapid hardening effect during the ageing was observed. They concluded that a high density of Mg–Cu cluster with high Mg:Cu ratio enhances the strengthening response.

The precipitation was proposed by Bagaraytsky in the early 40s, the discovery of new microscopy techniques has brought back the discussion of the existence of other phases. This precipitation sequence for the ageing of Al–Cu–Mg alloys as proposed by Bagaraytsky [4,5] is as follows:

$$\alpha\,(\text{supersaturated solid solution}) \rightarrow \text{GPB zones} \rightarrow S'' \rightarrow S' \rightarrow S \quad (1)$$

Perlitz and Westgren [6], working with X-ray diffraction (XRD), reported that the crystal structure of the equilibrium S-phase (Al_2CuMg) has an orthorhombic cell with space group Cmcm and lattice parameters $a_S = 0.400$ nm, $b_S = 0.923$ nm and $c_S = 0.714$ nm, and since then, these data have been widely used. This S-phase is coherent with the aluminium (Al) matrix, and therefore, the epitaxial relationships $(0\,1\,0)_S//(0\,2\,1)_{Al}$ and $[1\,0\,0]_S//[1\,0\,0]_{Al}$ is the most widely reported [7].

At present, many authors consider that the S′-phase is a slightly distorted version of stable S-phase and do not make any distinction between its orthorhombic structure [7], even though the main difference between these two phases is the degree of coherency with the matrix. Charai et al. [8] mentioned that there is a reasonable difference between the crystal parameters of the S-phase and the S′-phase and, therefore, they cannot be considered as the same phase. However, the lattice parameters proposed for the S′-phase strongly depend on the degree of coherency. In this sense, the main controversy is focused on the existence of the metastable S″-phase proposed by Bagaraytsky. A number of models have been suggested in order to support the existence of this phase or to refine its crystal structure, for instance, Cuisiat [10] observed an S″-phase with different structure given by Bagaraytsky. Shih et al. [11] proposed partially ordered GPB (Guinier–Preston–Bagaraytsky) zones. Charai et al. [8] suggested that the S″-phase originates from the agglomeration of GPB monolayers and has a monoclinic unit cell with parameters of $a_{S''} = 0.32$ nm, $b_{S''} = a_{Al}$ $c_{S''} = 0.254$ nm and $\beta = 91.7°$. Wang et al. [9] proposed an orthorhombic structure with Imm2 space group and cell parameters of $a_{S''} = b_{S''} = 0.405$ nm and $b_{S''} = 1.62$ nm.

Ringer et al. [12] reported that there is a possibility that the S″-phase could be explained as an orientation variant of the S-phase. This is due to the S-phase has 12 crystallography equivalent variants and the electron diffraction pattern identified as S″-phase is consistent with the S-phase when viewed from the $[0\,0\,1]_{Al}$ orientation (variant S_1). Recently, Kovarik [13,14], based on HRTEM image simulations, proposed that the electron diffraction pattern of the metastable S″-phase can be explained as an orientation variant

* Corresponding author.
E-mail address: joseggr@unam.mx (G. González).

0254-0584/$ – see front matter © 2011 Elsevier B.V. All rights reserved.
doi:10.1016/j.matchemphys.2011.07.004

of the equilibrium phase-S. The objective of this work is to provide more information of different orientations from those already reported in the literature [12–14] and to provide an alternative explanation for the experimental evidence previously used as support for the S″-phase, through HRTEM.

2. Experimental procedure

An aluminium (Al) alloy with the nominal composition Al–2.1Cu–1.25Mg (wt.%) was cast into ingots and cold rolled, homogenised and machined into discs of a thickness of ~1 mm. The samples obtained after this process were solution heat treated at 525 °C for 0.5 h in a molten salt bath. The selected solution temperature was lower than the critical dissolution temperature to avoid localised melting. After the solution treatment, the samples were quenched in water at room temperature, ~20 °C, then aged at 150 °C for four days and quenched in water. The HRTEM investigations were carried out in a JEOL 2010F microscope, operated at 200 kV and equipped with field emission gun. The specimens for HRTEM were mechanically ground to a thickness of ~0.2 mm, and then electrolytic polishing was performed on thin foils of 3 mm diameter using a Struers Tenupol. A small hole was made using a double jet of methanol and nitric acid solution with a ratio of 3:1 at ~−30 °C. Digital Micrograph software was used to analyse the images obtained by the HRTEM, whilst the image simulation was carried out with an electron microscope simulation (EMS) software. In the HRTEM simulations, the microscope parameter were: acceleration voltage = 200 kV, spherical aberration coefficient = 0.7 mm, beam convergence = 0.75 mrad and spread of defocus = 5 nm [15]. The "two overlapping networks method" (TONM) [16] was employed to visualise the Moiré patterns produced by the interference between the Al matrix and the equilibrium S-phase. This method consists of rotating two overlapped images of the studied network. The network overlapped can generate Moiré patterns. Another advantage of using this method is that almost all the contrasts observed in the experimental images can be reproduced.

3. Results and discussion

According to the reported epitaxial relationship, there are 12 resultant orientation variants between the Al matrix and the S-phase [17]. Fig. 1A–C shows the simulated electron diffraction patterns (SEDP) of 3 orientation variants (the other 9 variants are produced by the rotation of these 3 variants with respect to the Al lattice). In these simulated diffraction patterns, the gray spots correspond to Al lattice reflections, the black spots correspond to S-phase reflections and dark-gray spots are generated by double-diffraction. The simulated diffraction pattern shown in Fig. 1A has been identified as the characteristic diffraction pattern of the equilibrium S-phase and corresponds to the orientation variant I, where the zone axis is parallel to $[1\,0\,0]_S$. In Fig. 1B the simulated diffraction pattern corresponds to the orientation variant II, which has been reported as the metastable S″-phase, whereas the orientation variant III presented in the simulated diffraction pattern in Fig. 1C has not been identified as a different phase. Note that this orientation variant III, is precisely the one we are proposing as a key phase to clarify that there is no S″-phase and yet, it has not been named in the literature.

In order to understand the origin of these orientation variants, a diagram of the epitaxial relationship between the Al matrix and the S-phase is shown in Fig. 2A. According to this diagram, the (0 1 0) planes of the S-phase begin to grow under (0 2 1) Al planes, therefore, the resultant inclination of the S-phase with respect to horizontal axis is ~26.58°. According to Fig. 2A, if the view direction is orientated parallel to the $[1\,0\,0]_{Al}$ lattice, then the view direction will be parallel to the $[1\,0\,0]_S$, giving rise to the orientation variant I, as shown in Fig. 1A. On the other hand, if the view direction is parallel to the $[0\,1\,0]_{Al}$ lattice, then the view direction will be almost parallel to the $[0\,\bar{2}\,1]_S$, bringing about the orientation variant II. Considering the epitaxial relationship between Al and S-phase, the $[0\,\bar{2}\,1]_S$ have a misorientation (or geometric difference) of 5.75° with respect to the $[0\,1\,0]_{Al}$. However, if the view direction is parallel to the $[0\,0\,1]_{Al}$ lattice, then the view direction for S-phase is almost parallel to the $[0\,1\,3]_S$, giving rise to the orientation variant III, while the misorientation or geometric difference with respect to $[0\,0\,1]_{Al}$ is ~2.92°. Experimentally, the HRTEM images of the Al lattice obtained in the zone axes [1 0 0], [0 1 0] and [0 0 1] are identical. However, for the orthorhombic structure of the S-phase, the HRTEM images in the axes [1 0 0], $[0\,\bar{2}\,1]$ and [0 1 3] are completely different. The following sections explain, in detail, the experimental images, i.e. FFT and Fourier filters, of the 3 variants investigated for the Al–Cu–Mg alloy. Fig. 2B shows the schematic in 3D of the epitaxial relation, including the view directions that originated the variants mentioned above.

3.1. Variant I

Figs. 3–5A show the HRTEM images for the Al–Cu–Mg alloy aged at 150 °C for 4 days and Figs. 3–5B show the corresponding fast Fourier transform (FFT) at the regions shown in Figs. 3A–C. As can be observed, the FFT of these regions exhibit similar patterns to the diffraction patterns simulated for the orientation variants of the S-phase with respect to the Al lattice. The FFT in Fig. 3B which corresponds to the region showed in Fig. 3A is similar to the orientation variant I. As previously mentioned, this orientation variant has been identified as S-phase. Fig. 3D shows an inverse FFT when applying a Fourier filter over the Al reflections; here, the HRTEM image expected for Al lattice in the zone axis [1 0 0] is observed. Similarly, Fig. 3C shows the inverse FFT when applying a Fourier filter over the precipitate reflections, so that the Al matrix is then removed in order to show clearly the structure of the precipitates.

3.2. Variant II

With regard to variant II, Fig. 4B shows the FFT of the region observed in the HRTEM image shown in Fig. 4A. This pattern has already been identified in the literature as the metastable S″-phase and it is similar to the simulated diffraction pattern obtained for the orientation variant II in Fig. 1B. With the HRTEM image displayed in Fig. 4A, it is *not* possible to observe a clear contrast arising from the precipitate; therefore, a Fourier filter was applied over the Al lattice reflections where the inverse FFT is similar to the one observed in Fig. 3D. When the Fourier filter is applied over the precipitate reflections, the pattern on the inverse FFT (Fig. 4C) is different from the pattern obtained for the Al lattice. If the analysis were to stop here, the confusion/controversy of the existence of the metastable S″-phase would continue, since this slight change between the two lattices can generate a Moiré interference pattern that can be confused with the presence of other phases i.e. S″. It is worth mentioning that variants I and II were already reported by Ringer et al. [12] and Kovarik et al. [13,14], therefore, it is imperative to include a third variant, which will observe the structure from a different zone axis in order to contribute to the clarification of the aforementioned confusion/controversy.

3.3. Variant III

As mentioned above, the introduction of the variant III proved to be very important in identifying the nature of the so-called S″-phase in the Al–Mg–Cu alloys. From the FFT in Fig. 5B, which corresponds to the region shown in Fig. 5A, it can be observed that this pattern is similar to that simulated of the orientation variant III in Fig. 1C. In the HRTEM image, it is possible to detect a contrast that arises from the precipitate, but only when the FFT is calculated, an additional lattice is detected. Then, when applying a Fourier filter to the reflections of the Al lattice, a similar inverse FFT image is observed, as shown in Fig. 3D. In order to identify the crystalline lattice that produced the additional spots in the FFT pattern (Fig. 5B), a Fourier filter was applied over the additional reflected spots, and then the inverse FFT was calculated, as shown in Fig. 5C. With this FFT, the crystalline lattice is clearly observed in comparison with

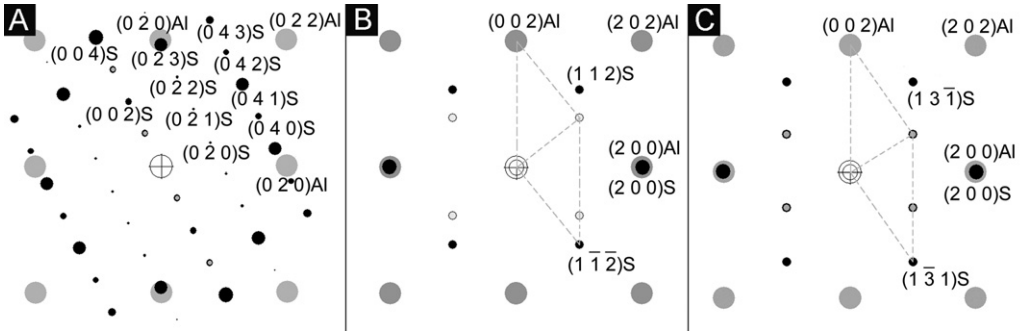

Fig. 1. Simulated electron diffraction patterns corresponding to the orientation variants of S-phase pertaining to the Al matrix. (A) Variant I, (B) variant II and (C) variant III.

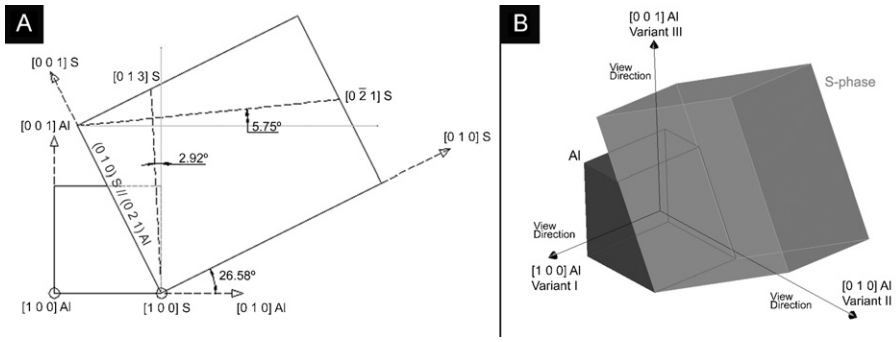

Fig. 2. (A) Projection of the Al and S-phase lattices according to the epitaxial relationship (0 2 1)Al//(0 1 0)S; [1 0 0]Al//[1 0 0]S, and (B) 3D view of the epitaxial relationship of the S-phase and Al matrix.

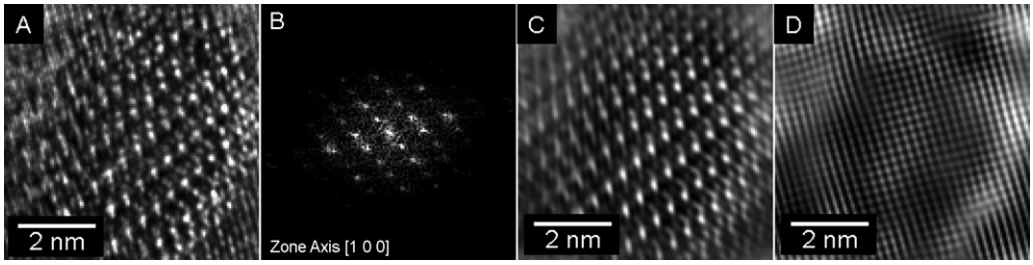

Fig. 3. (A) HRTEM image corresponding to the Variant I of the S-phase in Al–Cu–Mg alloy aged at 150 °C for 4 days, (B) FFT obtained from (A), (C) HRTEM image of (A) after applying a Fourier Filter over the precipitate reflections, and (D) HRTEM image of (A) after applying a Fourier Filter over the Al matrix reflections.

the previous variants where the contrast could be wrongly taken as a different phase. Therefore, the introduction of this variant clarifies that the S″-phase in Al–Cu–Mg alloys might be understood as a contrast effect of the interference of Al and S-phase lattices.

In order to explain the influence of the planes that are involved in the formation of the image, the contrast transfer function (CTF) of the microscope employed in this work was calculated. In the case of the Al lattice oriented in zone axes [1 0 0], only the planes (2 0 0) and (2 2 0) are involved in the formation of the image, but only the (2 0 0) plane appears before the first intersection with the *X*-axis, commonly known as point-to-point resolution (Fig. 6A), for this reason, the HRTEM images of Al in zone axis [1 0 0] do display a poor contrast. For the S-phase in the same zone axis, before the first intersection with the *X*-axis, at least 8 planes participate in the formation of images, as shown in Fig. 6B; consequently, the HRTEM images have high contrast and, therefore, a good definition. Similar

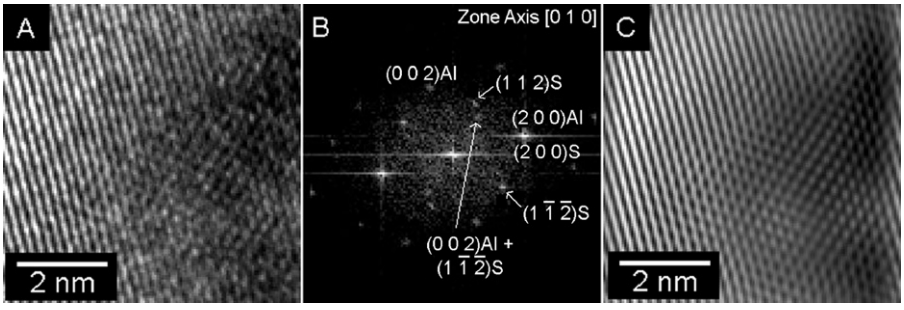

Fig. 4. (A) HRTEM image corresponding to the Variant II of the S-phase in Al–Cu–Mg alloy aged at 150 °C for 4 days, (B) FFT obtained from (A), (C) HRTEM image of (A) after applying a Fourier Filter over the precipitate reflections.

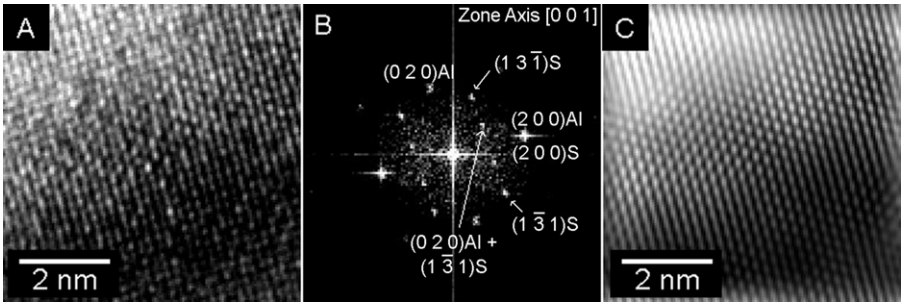

Fig. 5. (A) HRTEM image corresponding to the Variant III of the S-phase in Al–Cu–Mg alloy aged at 150 °C for 4 days, (B) FFT obtained from (A), (C) HRTEM image of (A) after applying a Fourier filter over the precipitate reflections.

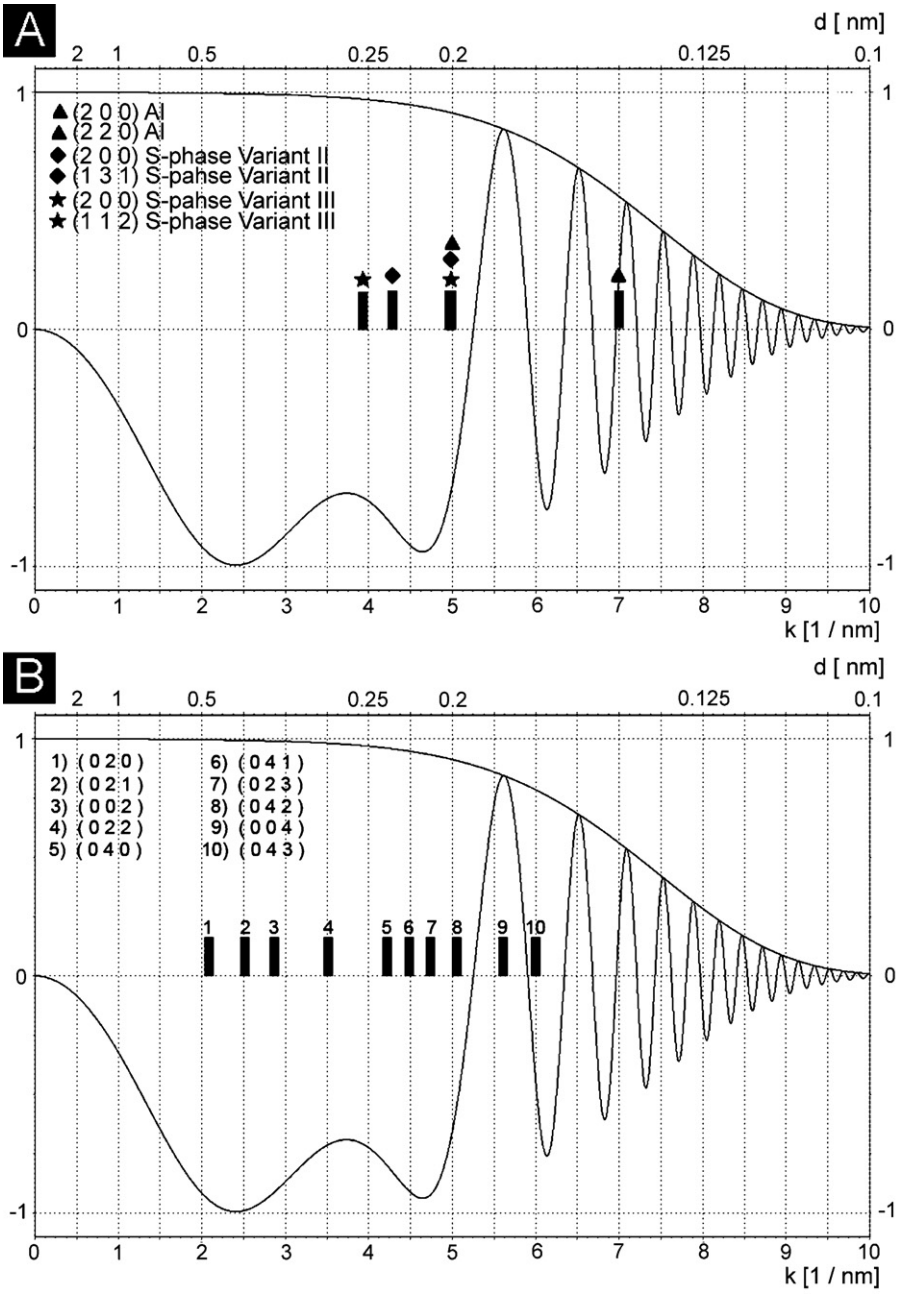

Fig. 6. Contrast transfer function (CTF) of JEOL 2010F microscope showing the interplanar distances for: (A) Al, variant II and variant III, and (B) variant I.

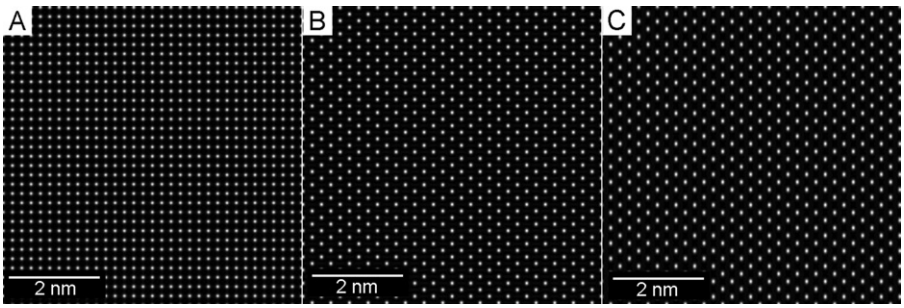

Fig. 7. Simulated HRTEM image using the multislice method on: (A) Al lattice in the [1 0 0] zone axis, (B) S-phase in zone axes [0 $\bar{2}$ 1] and (C) S-phase in zone axes [0 1 3].

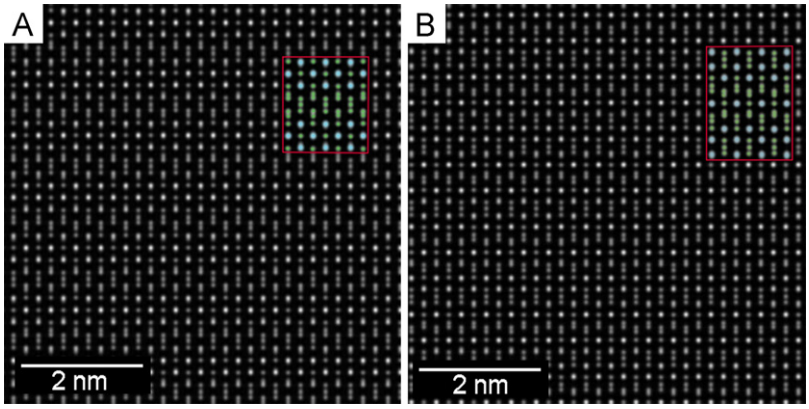

Fig. 8. (A) Image obtained when superimposing Fig. 7A with Fig. 7B, and (B) image obtained when superimposing Fig. 7A with Fig. 7C.

observations were found for the S-phase in zone axes [0 $\bar{2}$ 1] and [0 1 3] (Fig. 6A). This complicates the interpretation of these images, as the Al in zone axis [1 0 0] as well as the S-phase on these axes have similar contrast, making difficult the interpretation of images, since S-phase is embedded in the Al matrix.

To understand the experimental HRTEM images, the simulated S-phase images in the zone axes [0 $\bar{2}$ 1] and [0 1 3] and the Al in zone axis [1 0 0] were obtained. In the simulated image of Al in Fig. 7A, it is observed that the array of spots is similar to the array observed in the experimental image. Fig. 7B, which corresponds to the simulated image of the orientation variant II, exhibits an array of spots similar to the array presented in the filtered experimental image of Fig. 4C, whereas in the simulated images of the orientation variant III shown in Fig. 7C, the array of spots is almost equal to the array observed in the filtered experimental image of Fig. 5C. In the real case, the precipitates are embedded in the Al matrix, and therefore, the experimental image is formed by the interference of two lattices; this interference can produce Moiré patterns as previously mentioned. To explain the interaction between matrix and precipitate, the simulated image of Al and the S-phase were overlapped, using the TONM, in the orientation variants II and III. The resultant image clearly shows (Fig. 8A) the interference of the Al lattice with the S-phase in the orientation variant II, and it was observed that the Moiré pattern generated is similar to the image reported in the literature as S″-phase. Thus, the Moiré pattern generated by the interference of Al and S-phase in orientation variant III (Fig. 8B) is not clear but the image generated is quite similar to the image in Fig. 5A.

The introduction of variant III combined with the TONM to analyse the interaction between the Al matrix and S-phase proved to be very useful, as it was possible to clarify by HRTEM the true nature of the commonly known metastable S″-phase. Since the interference between the Al and S-phase normally generates Moiré patterns, the S″-phase could be easily misinterpreted as a different metastable phase. However, with the results mentioned above, it was possible to identify that the S″-phase is just a visual effect generated by the interference between the Al matrix and the equilibrium S-phase.

Therefore, the precipitation of Al–Cu–Mg alloys could have the following sequence:

$$\alpha\ (\text{supersaturated solid solution}) \rightarrow \text{GPB zones} \rightarrow S' \rightarrow S \qquad (2)$$

Finally, the other techniques such as differential scanning calorimetry, that have reported the existence of the S″-phase should be reassessed, taking into account this new evidence.

4. Conclusions

According to the epitaxial relationship between the aluminium (Al) matrix and the S-phase, there are 12 resultant orientation variants. As there is no restriction for the preferential growth of the S-phase variants, any of these could co-exist. The experimental evidence showed that the reflexions in the FFT could be explained as an orientation variant of the equilibrium S-phase, and the extra spots that appeared in the FFT are associated with double diffraction effect. The incorporation of variant III, which has not been reported in the literature using HRTEM, strongly suggests that the S-phase could co-exist in any of these variants. The S-phase in the zone axis [0 $\bar{2}$ 1] does not have a good contrast and the interference between the Al matrix generates a Moiré interference pattern that can be confused with the presence of other phase, such as the so-called S″-phase. The combination of variant III and the "two overlapping networks method" allowed us to propose that there is no S″-phase, and that the effects attributed to S″ are explained by consideration of the various variants of the equilibrium S phase. In consequence, from the aforementioned results, the reinterpretation of the differential scanning calorimetry results reported in

the literature and the reassessment of the precipitation sequences and hardening mechanisms in Al–Cu–Mg alloys will be necessary.

Acknowledgments

The authors are grateful for the financial support of CONACyT and PAPIIT-UNAM through grant No. IN112010. Adriana Tejeda, Carlos Flores Morales and Erika Contreras are also acknowledged for their valuable technical assistance.

References

[1] P.J. Gregson, H.M. Flower, Microstructural control of toughness in aluminium–lithium alloys , Acta Metall. 33 (1985) 527–537.
[2] S.P. Ringer, T. Sakurai, I.J. Polmear, On the origins of hardening in Al–Cu–Mg–(Ag) alloys , Acta Mater. 45 (1997) 3731–3744.
[3] R.K.W. Marceau, G. Sha, R. Ferragut, A. Dupasquier, S.P. Ringer, Solute clustering in Al–Cu–Mg alloys during the early stages of elevated temperature ageing , Acta Mater. 58 (2010) 4923–4939.
[4] Y.A. Bagaraytsky, Mechanism of artificial ageing of Al–Cu–Mg alloy , Dokl. Akad. Nauk SSSR 87 (1952) 397–400.
[5] Y.A. Bagaraytsky, Characteristics of natural ageing of aluminum alloy , Dokl. Akad. Nauk SSSR 87 (1952) 559–562.
[6] H. Perlitz, A. Westgren, The crystal structure of Al_2CuMg , Arkiv. Kemi. Mineral Geol. 16B (1943) 1–8.
[7] J.M. Silcock, The structural ageing characteristics of Al–Cu–Mg alloys with copper:magnesium weight ratios of 7:1 and 2.2:1 , J. Inst. Met. 89 (1960–1961) 203–210.
[8] A. Charai, T. Walther, C. Alfonso, A.-M. Zahra, C.Y. Zahra, Coexistence of clusters, GPB zones S″-, S′- and S-phases in an Al–0.9% Cu–1.4% Mg alloy , Acta Mater. 48 (2000) 2751–2764.
[9] S.C. Wang, M.J. Starink, The assessment of GPB2/S″ structures in Al–Cu–Mg alloys , Mater. Sci. Eng. A 386 (2004) 156–163.
[10] F. Cuisiat, P. Duval, R. Graf, Etude des premiers stades de décomposition d'un alliage Al–Cu–Mg , Scripta Metall. 18 (1984) 1051–1056.
[11] H.-C. Shih, N.-J. Ho, J.C. Huang, Precipitation behaviours of Al–Cu–Mg and 2024 aluminium alloys , Metall. Mater. Trans. A27 (1996) 2479–2494.
[12] S. Ringer, S.K. Caraher, I. Polmear, Response to comments on cluster hardening in an aged Al–Cu–Mg alloy , Scripta Mater. 39 (1998) 1559–1567.
[13] L. Kovarik, S.A. Court, M.J. Mills, HRTEM observations and simulations of the S″-phase in Al–Mg–Cu alloys and its implications for Al–Cu–Mg alloys , in: Proceedings of the 9th International Conference on Aluminium Alloys (ICAA9), 2004, pp. 736–741.
[14] L. Kovarik, M.K. Miller, S.A. Court, M.J. Mills, Origin of the modified orientation relationship for S(S″)-phase in Al–Mg–Cu alloys , Acta Mater. 54 (2006) 1731–1740.
[15] P. Stadelmann, EMS – a software package for electron diffraction analysis and HREM image simulation in materials science , Ultramicroscopy 21 (1987) 131–145.
[16] J. Reyes-Gasga, S. Tehuacanero, M. José Yacamán, Moiré patterns in high resolution electron microscopy images of MoS_2 , Microsc. Res. Tech. 40 (1998) 2–9.
[17] S.C. Wang, M.J. Starink, Precipitates and intermetallic phases in precipitation hardening Al–Cu–Mg–(Li) based alloys , Inter. Mater. Rev. 50 (2005) 193–215.